Finite Elasto-Plasto-Dynamics – Challenges & Solutions

Rouven Mohr[1], Andreas Menzel[2,3], and Paul Steinmann[4]

[1] University of Kaiserslautern
Chair of Applied Mechanics
Department of Mechanical and Process Engineering
D-67653 Kaiserslautern, Germany
rmohr@rhrk.uni-kl.de

[2] Dortmund University of Technology
Group of Mechanics and Machine Dynamics
Faculty of Mechanical Engineering
D-44227 Dortmund, Germany
andreas.menzel@udo.edu

[3] Lund University
Division of Solid Mechanics
SE-22100 Lund, Sweden
andreas.menzel@solid.lth.se

[4] University of Erlangen-Nuremberg
Institute of Applied Mechanics
Department of Mechanical Engineering
D-91058 Erlangen, Germany
paul.steinmann@ltm.uni-erlangen.de

Abstract: In this contribution, we deal with time-stepping schemes for geometrically nonlinear multiplicative elasto-plasto-dynamics. Thereby, the approximation in space as well as in time rely both on a Finite Element approach, providing a general framework which conceptually includes also higher-order schemes. In this context, the algorithmic conservation properties of the related integrators strongly depend on the numerical computation of time integrals, particularly, if plastic deformations are involved. However, the application of adequate quadrature rules enables a fulfilment of physically motivated balance laws and, consequently, the consistent integration of finite elasto-plasto-dynamics. Using exemplarily linear Finite Elements in time, the resulting integration schemes are analysed regarding the obtained conservation properties and assessed in comparison to classical time-stepping schemes which commonly adopt a time-discretisation procedure based on Finite Differences.

1 Introduction

On the one hand, computational modelling of materials and structures often demands the incorporation of inelastic and dynamic effects. On the other hand, the performance of classical time integration schemes for structural dynamics, as for instance developed in [HHT77, New59], is strongly restricted when dealing with highly nonlinear systems. In a nonlinear setting, advanced numerical techniques are required to satisfy the classical balance laws as for instance balance of linear and angular momentum or the classical laws of thermodynamics. Nowadays, energy and momentum conserving time integrators for dynamical systems, like multibody systems or elasto-dynamics, are well-established in the computational dynamics community, compare e.g. [BB99, BBT01a, BBT01b, Gonz00, KC99, ST92]. In contrast to the commonly used time discretisation based on Finite Differences, one-step implicit integration algorithms relying on Finite Elements in space and time were developed, for instance, in Betsch and Steinmann [BS00a, BS00b, BS01]. Therein, conservation of energy and angular momentum have been shown to be closely related to quadrature formulas required for numerical integration in time. Furthermore, specific algorithmic energy conserving schemes for hyperelastic materials can be based on the introduction of an enhanced stress tensor for time shape functions of arbitrary order, compare Gross *et al.* [GBS05]. However, most of the proposed approaches are restricted to conservative dynamical systems. Nevertheless, the consideration of plastic deformations in a dynamical framework, involving dissipation effects, is of cardinal importance for various applications in engineering. In the last years, notable contributions dealing with finite elasto-plasto-dynamics have been published by Meng and Laursen [ML02a, ML02b], Noels *et al.* [NSP06] and Armero [Arm05, Arm06, AZ06]. In this contribution, we follow the concepts which have been proposed for hyperelasticity in [BS01, GBS05] and pick-up the general framework of Galerkin methods in space and time, developing integrators for finite multiplicative elasto-plasto-dynamics with pre-defined conservation properties, compare Mohr *et al*. [MMS06a, MMS07c, MMS07a, MMS07b]. By means of a representative numerical example, the excellent performance of the resulting schemes, which base on linear Finite Elements in time combined with different quadrature rules, will be demonstrated and compared with the performance of well-accepted standard integrators.

2 Semi-Discrete Dynamics

To set the stage, we start with some basic notation of geometrically nonlinear continuum mechanics. First, the nonlinear deformation map $\boldsymbol{\varphi}(\boldsymbol{X}, t) : \mathcal{B}_0 \times [0, T] \rightarrow \mathcal{B}_t$ shall be introduced as a mapping from the reference to the spatial configuration. As proposed by Lee [Lee69], the resulting deformation gradient $\boldsymbol{F} := \nabla_{\boldsymbol{X}} \boldsymbol{\varphi}(\boldsymbol{X}, t)$ is assumed to be multiplicatively decomposed into an elastic and a plastic part

$$\boldsymbol{F} \doteq \boldsymbol{F}_e \cdot \boldsymbol{F}_p \,, \tag{1}$$

implying an additional intermediate configuration related to purely plastic deformations, as illustrated in Fig. 1. In contrast to the modelling of elasticity, additional internal variables

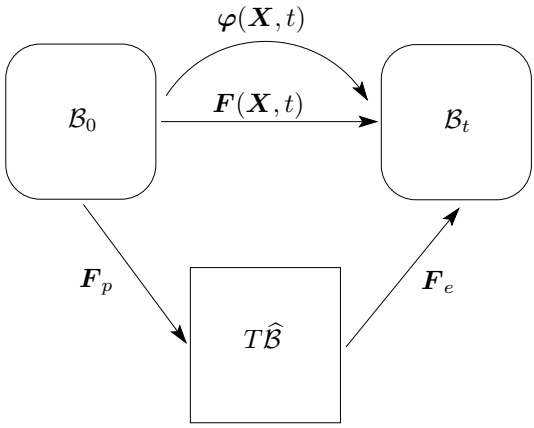

Figure 1: Resulting configurations within the framework of finite multiplicative plasticity

are included in the Helmholtz energy density ψ for the plastic case to model the loading history. By assuming an additive structure and elastic isotropy, the Helmholtz energy density ψ can be written in terms of the eigenvalues ${}^{i}\lambda_{\widehat{\boldsymbol{C}_e}}$ of the elastic right Cauchy-Green strain tensor

$$\widehat{\boldsymbol{C}_e} := \boldsymbol{F}_e^{\mathrm{t}} \cdot \boldsymbol{F}_e \tag{2}$$

of the intermediate configuration and the internal variables $\boldsymbol{\kappa} = [\boldsymbol{\kappa}^{mac}, \boldsymbol{\kappa}^{mic}]$

$$\psi(\boldsymbol{F}, \boldsymbol{\kappa}) = \psi^{mac}({}^{1}\lambda_{\widehat{\boldsymbol{C}_e}}, {}^{2}\lambda_{\widehat{\boldsymbol{C}_e}}, {}^{3}\lambda_{\widehat{\boldsymbol{C}_e}}) + \psi^{mic}(\boldsymbol{\kappa}^{mic})\,. \tag{3}$$

For thermodynamical aspects, it is accepted to introduce the so-called conjugated thermodynamical forces $\boldsymbol{\beta} := -\nabla_{\boldsymbol{\kappa}}\psi$. To differ between elastic and plastic deformation states, the yield function Φ is introduced which defines the elastic range $\mathbb{E}_{\boldsymbol{\beta}} := \{\boldsymbol{\beta} \,|\, \Phi(\boldsymbol{\beta}; \boldsymbol{\kappa}) < 0\}$. In view of thermodynamically consistent modelling, the dissipation inequality – corresponding to the second law of thermodynamics – should be fulfilled, namely

$$\mathcal{D} = \left\langle \boldsymbol{\beta}, \dot{\boldsymbol{\kappa}} \right\rangle \quad \geq 0\,. \tag{4}$$

For more detailed information, we refer to Simo [Sim98]. Subsequently, we apply a standard Finite Element discretisation in space for the reference configuration of a solid continuum body. Using the spatial approximations for the nonlinear deformation map, the semi-discrete map $\boldsymbol{\varphi} : \mathcal{B}_0 \times [0, T] \rightarrow \mathbb{R}^{n_{dim}}$ can be written by means of the spatial shape functions $N_A(\boldsymbol{X})$ in the form:

$$\boldsymbol{\varphi}(\boldsymbol{X}, t) \approx \sum_{A=1}^{n_{node}} \boldsymbol{q}_A(t)\, N_A(\boldsymbol{X}) \tag{5}$$

Consequently, the approximations in space of the spatial velocity $\boldsymbol{v} := \sum_{A=1}^{n_{node}} \dot{\boldsymbol{q}}_A \, N_A$, the deformation gradient $\boldsymbol{F} = \sum_{A=1}^{n_{node}} \boldsymbol{q}_A \otimes \nabla_{\boldsymbol{X}} N_A$, and the right Cauchy-Green strain tensor

$$\boldsymbol{C} := \boldsymbol{F}^{\mathrm{t}} \cdot \boldsymbol{F} = \sum_{A,B=1}^{n_{node}} \boldsymbol{q}_A \cdot \boldsymbol{q}_B \, \nabla_{\boldsymbol{X}} N_A \otimes \nabla_{\boldsymbol{X}} N_B \tag{6}$$

can be computed straightforwardly. To obtain a semi-discrete system of equations of motion, we combine the placements of the spatial nodes $\boldsymbol{q} = [\boldsymbol{q}_1, ..., \boldsymbol{q}_{n_{node}}]^{\mathrm{t}}$ and the nodal generalised momenta $\boldsymbol{p} := \mathbb{M} \cdot \dot{\boldsymbol{q}} = [\boldsymbol{p}_1, ..., \boldsymbol{p}_{n_{node}}]^{\mathrm{t}}$ to a vector of the canonical phase-space variables $\boldsymbol{z} := [\boldsymbol{q}, \boldsymbol{p}]^{\mathrm{t}}$. Furthermore, the kinetic and free energy

$$T(\boldsymbol{p}) = \frac{1}{2} \, \boldsymbol{p} \cdot \mathbb{M}^{-1} \cdot \boldsymbol{p} \qquad \text{respectively} \qquad \Psi = \int_{\mathcal{B}_0} \psi \, \mathrm{d}V \tag{7}$$

are introduced for the semi-discrete case. Motivated by the well-known Hamiltonian H for conservative systems, the sum consisting of kinetic energy, free energy, and possibly an external potential V^{ext} will be denoted by

$$H(\boldsymbol{q}, \boldsymbol{p}; \boldsymbol{\kappa}) = T + \Psi + V^{ext} \, . \tag{8}$$

Dealing with dissipative systems, the global accumulated dissipation

$$D := \int_{\mathcal{B}_0} d \, \mathrm{d}V \qquad \text{based on} \qquad d := \int_0^t \mathcal{D} \, \mathrm{d}t \tag{9}$$

has to be taken into account. Analogously to the purely elastic case, the resulting (canonical) equations of motion can still be written in a compact format of the Hamiltonian-type

$$\dot{\boldsymbol{z}}(t) = \mathbb{J} \cdot \nabla_{\boldsymbol{z}} H(\boldsymbol{z}; \boldsymbol{\kappa}) \qquad \text{with} \qquad \mathbb{J} = \begin{bmatrix} \boldsymbol{0} & \boldsymbol{I} \\ -\boldsymbol{I} & \boldsymbol{0} \end{bmatrix} , \tag{10}$$

representing a system of ordinary differential equations of first order. Therein, the gradient with respect to the global variables $\boldsymbol{z}$ can be specified by

$$\nabla_{\boldsymbol{z}} H = \begin{bmatrix} \boldsymbol{F}^{int} - \boldsymbol{F}^{ext} \\ \\ \mathbb{M}^{-1} \cdot \boldsymbol{p} \end{bmatrix} , \tag{11}$$

involving the definition of the internal load vector

$$\boldsymbol{F}^{int}(\boldsymbol{S}) := \nabla_{\boldsymbol{q}} \int_{\mathcal{B}_0} \psi \, \mathrm{d}V \tag{12}$$

based on the Piola Kirchhoff stresses $\boldsymbol{S} = 2 \, \nabla_{\boldsymbol{C}} \, \psi$. In the following, especially this highly nonlinear internal load vector plays a crucial role with regard to the discretisation in time and, consequently, concerning the resulting conservation properties of the Galerkin-based time-stepping schemes.

3 Discretisation in Time

As mentioned above, in the proposed concept not only the approximation in space but also the approximation in time relies on a Finite Element approach, see also [BS00b, Bot97, EEHJ96]. We start with a decomposition of the time interval $[0,T] = \bigcup_{n=0}^{N} [t_n, t_{n+1}]$ and a map of each sub-interval to the reference time interval $[0,1]$ via the function $\alpha(t) := [t - t_n]/h_n$, involving the time-step size $h_n = t_{n+1} - t_n$. For the time approximation, a continuous Galerkin method (or short: a 'cG(k) method') shall be applied. Therefore, the approximations in time for the unknown and the test function

$$\boldsymbol{z}^h = \sum_{j=1}^{k+1} M_j(\alpha)\, \boldsymbol{z}_j \qquad\qquad \delta\boldsymbol{z}^h = \sum_{i=1}^{k} \widetilde{M}_i(\alpha)\, \delta\boldsymbol{z}_i \tag{13}$$

are introduced [1]. In a compact notation the resulting weak form in time is given by the integral

$$\int_0^1 \left[\mathbb{J} \cdot \delta\boldsymbol{z}^h\right] \cdot \left[\mathrm{D}_\alpha \boldsymbol{z}^h - h_n\, \mathbb{J} \cdot \nabla_{\boldsymbol{z}} H(\boldsymbol{z};\boldsymbol{\kappa})\right] \mathrm{d}\alpha = 0\,. \tag{14}$$

Inserting the approximations in time (13) in Eq. (14) renders the discrete system of equations of motion

$$\sum_{j=1}^{k+1} \int_0^1 \widetilde{M}_i M_j^{'}\, \mathrm{d}\alpha\; \boldsymbol{z}_j - h_n \mathbb{J} \cdot \int_0^1 \widetilde{M}_i\, \nabla_{\boldsymbol{z}} H(\boldsymbol{z};\boldsymbol{\kappa})\, \mathrm{d}\alpha = \boldsymbol{0} \qquad \forall\ i = 1, ..., k \tag{15}$$

involving a time-integrated internal load vector. Thereby, higher-order integration schemes are included within this general framework. Further details can be found in Betsch and Steinmann [BS01]. Dealing with time-stepping schemes, special emphasis should be always placed on resulting algorithmic conservation properties which strongly influence the numerical performance. In this context, it is often desirable to transfer as many as possible of the conservation properties from the continuous to the completely discrete system, especially, regarding the underlying physics and the robustness of the related integration scheme. For the proposed concept, the approximation of the time-integrated internal load vector

$$\bar{\boldsymbol{F}}_i^{int} := \int_0^1 \widetilde{M}_i(\alpha)\, \boldsymbol{F}^{int}(\boldsymbol{S})\, \mathrm{d}\alpha \qquad \text{with} \qquad i = 1, ..., k \tag{16}$$

is the crux concerning the offered conservation properties of Galerkin-based time-stepping schemes. In fact, integrators with pre-defined conservation properties can be designed, adjusting the applied quadrature rule.

[1] It is important to emphasise that the time shape functions $M_j \in \mathcal{P}^k$ are polynomials of degree k, whereas the reduced shape functions $\widetilde{M}_i \in \mathcal{P}^{k-1}$ are only of degree $k-1$.

3.1 Standard quadrature

Involving $\boldsymbol{I} = \sum_{A=1}^{n_{node}} \boldsymbol{p}_A$ and $\boldsymbol{L} = \sum_{A=1}^{n_{node}} \boldsymbol{q}_A \times \boldsymbol{p}_A$, the application of a standard Gauss quadrature rule for the approximation of the time integral given by Eq. (16) already enables the conservation of both momentum maps (for vanishing external loads)

$$\boldsymbol{I}_{\alpha=1} - \boldsymbol{I}_{\alpha=0} = \boldsymbol{0} \qquad\qquad \boldsymbol{L}_{\alpha=1} - \boldsymbol{L}_{\alpha=0} = \boldsymbol{0}\,, \tag{17}$$

if an adequate number of integration points in time is incorporated, compare Betsch and Steinmann [BS01]. Nevertheless, an additional conservation of the total energy for elastic deformations, for instance, cannot be generally offered by means of such a standard quadrature rule. Moreover, the incorporation of physical dissipation effects related to plastic deformations poses further challenges for the applied quadrature rule. To tackle potential problems concerning algorithmic conservation properties, nonstandard quadrature rules must be taken into account.

3.2 Nonstandard quadrature

First, a nonstandard quadrature rule is introduced to guarantee the thermodynamical consistency of the integrator, in addition to the mechanical consistency which includes the conservation of both momentum maps corresponding to Eq. (17). Thermodynamically consistent integrators for elasto-plasto-dynamics are characterised by the conservation of the total energy in the elastic case

$$H_{\alpha=1} - H_{\alpha=0} = 0 \qquad \text{with} \qquad \Delta D = 0 \tag{18}$$

and by the (strictly) positive dissipation for plastic deformations represented by

$$H_{\alpha=1} - H_{\alpha=0} < 0 \qquad \text{combined with} \qquad \Delta D > 0\,, \tag{19}$$

compare Mohr *et al.* [MMS06a]. Finally, the application of an appropriate nonstandard quadrature rule renders energy-consistent Galerkin-based time-stepping schemes [2]. Thereby, energy-consistency includes the conservation of the sum consisting of the total energy and the dissipation represented by

$$H_{\alpha=1} - H_{\alpha=0} = -\Delta D \tag{20}$$

for elastic ($\Delta D = 0$) as well as for plastic ($\Delta D > 0$) deformations, whereby the fulfilment of Eq. (20) can be offered within the calculation accuracy. Detailed background informations concerning the consistency of a Galerkin-based integration of finite elasto-plasto-dynamics and corresponding technical details, like for instance the local integration of the plastic evolution equations, are presented in Mohr *et al.* [MMS07c].

[2] In the following, the thermodynamically consistent and mechanically consistent cG method will be referred to as 'TCMC-cG method' and the energy-consistent, mechanically consistent scheme as 'ECMC-cG method' to abbreviate the notation.

4 Numerical Examples

In this section, the performance of the outlined Galerkin-based concepts is analysed by means of a representative numerical example, evaluating the featured algorithmic conservation properties for the elastic as well as for the plastic case. As an appropriate example, the free motion of a 'Flying Frame' with the mass density ρ, consisting of 48 isoparametric 4-node elements in space, will be investigated. To start the free flight, the frame is equipped with a given initial velocity $||\boldsymbol{v}_0|| = 85$ and, furthermore, some external loads $\boldsymbol{F}^{ext}$ are applied during the loading period T_{load}. Thereby, the norm of the external load vector $||\boldsymbol{F}_A^{ext}|| = f(t)$ (at the spatial node A) is prescribed by the piecewise linear function $f(t)$ with the maximum value f_{max}, as illustrated in Fig. 2 a). For the following computations, linear Finite Elements in time have been applied as a fundamental example. The constitutive law relies on a Helmholtz energy density ψ of the Hencky-type with the material parameters λ, μ and on a v. Mises-type yield function Φ, involving the yield stress Y_0 and the modulus of linear isotropic hardening H.

4.1 Standard vs. nonstandard quadrature

First, the differences between the abovementioned standard and nonstandard quadrature rule for the approximation of the time-integrated internal load vector (16) will be studied in detail, regarding the purely elastic as well as the plastic case. In this context, a standard cG(1) method is compared with the 'TCMC-cG(1) method' respectively the 'ECMC-cG(1) method'. For the present computations, we have incorporated the parameters $\lambda = 10\,000$, $\mu = 5000$, $Y_0 = \infty|500$, $H = 500$, $\rho = 5.0$, $f_{max} = 100$, $T_{load} = 1.0$, and $h_n = 0.1$. Some snapshots of the motion are pictured in Fig. 2 b), whereby the plastic motion is displayed below the elastic case. The global accumulated dissipation D is, as

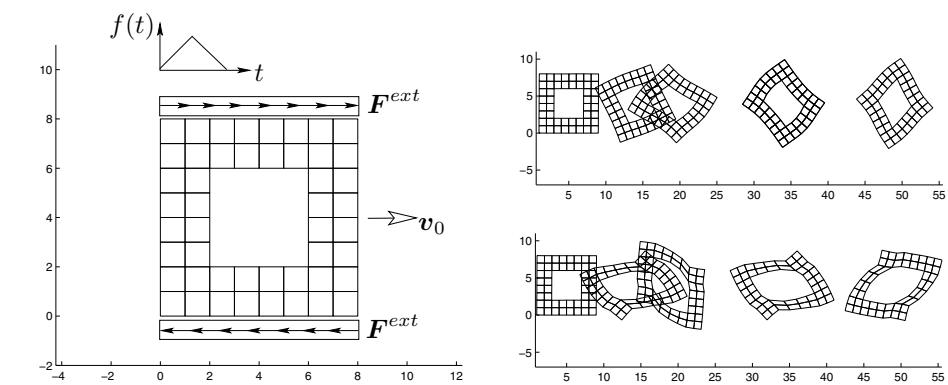

Figure 2: Configurations: a) initial mesh, b) sequence of the motion (elastic & plastic case) for $t \in \{0.1, 10, 15, 30, 45\}$

expected, equal to zero for each of the considered Galerkin-based integrators if the deformations are purely elastic, and it is (strictly) positive if plastic deformations are involved due to the application of an adequate local update algorithm for the plastic variables, compare Fig. 4. Furthermore, it can be clearly seen in Fig. 6 that mechanical consistency, related to a conservation of both momentum maps, can be guaranteed not only for time-stepping schemes which base on nonstandard quadrature rules, but also for the classical cG method which adopts a standard Gauss quadrature rule. Nevertheless, the influence of the applied quadrature rule becomes obvious when a plot of the total energy H is considered, as displayed in Fig. 3. In the elastic case, the total energy calculated by means of the standard cG method is characterised by strong oscillations, whereas the 'TCMC-cG method' as well as the 'ECMC-cG method' guarantee both the conservation of the total energy. Moreover, the cG method features an unphysical increase of the total energy in the plastic case. Contrariwise, both schemes based on nonstandard quadrature rules guarantee a monotonic decrease of the total energy caused by the (strictly) non-negative plastic dissipation. However, a physically correct decrease of the total energy H respectively increase of the dissipation D – related to a conservation of the augmented Hamiltonian $H + D$ – is guaranteed exclusively by the 'ECMC-cG method', as illustrated in Fig. 5.

4.2 Standard vs. nonstandard integrator

Finally, the performance of the proposed Galerkin-based integration schemes, represented by the 'ECMC-cG method', will be compared with the results calculated by means of standard time integration schemes. In this context, we have exemplarily chosen two of the most-established integrators at all: the classical Newmark scheme with $\gamma = 0.5$, $\beta = 0.25$ and the Hilber-Hughes-Taylor method (abbreviated by 'HHT method') with the parameters $\gamma = 0.8$, $\beta = 0.422$, and $\alpha = -0.30$, as proposed in [Hug87]. Both standard integrators have been developed originally for linear dynamical systems, whereby

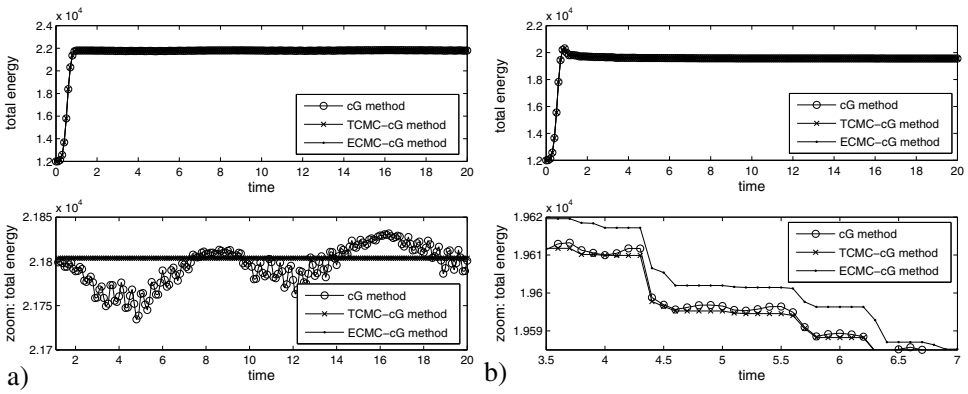

Figure 3: Total energy H: a) purely elastic case, b) plastic case

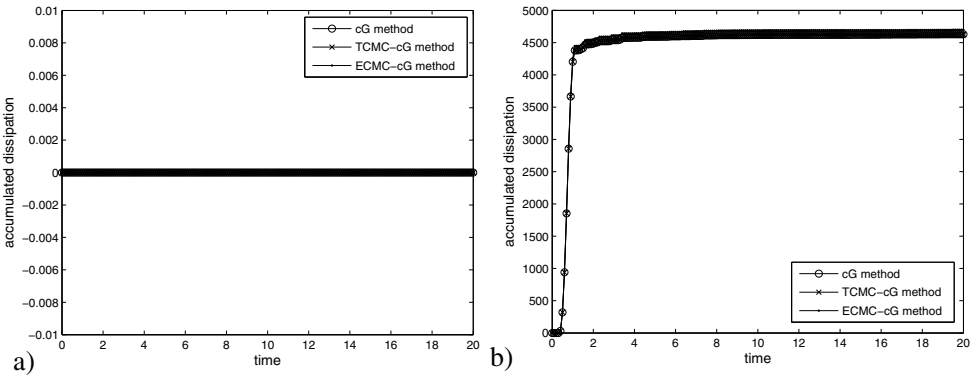

Figure 4: Accumulated dissipation D: a) purely elastic case, b) plastic case

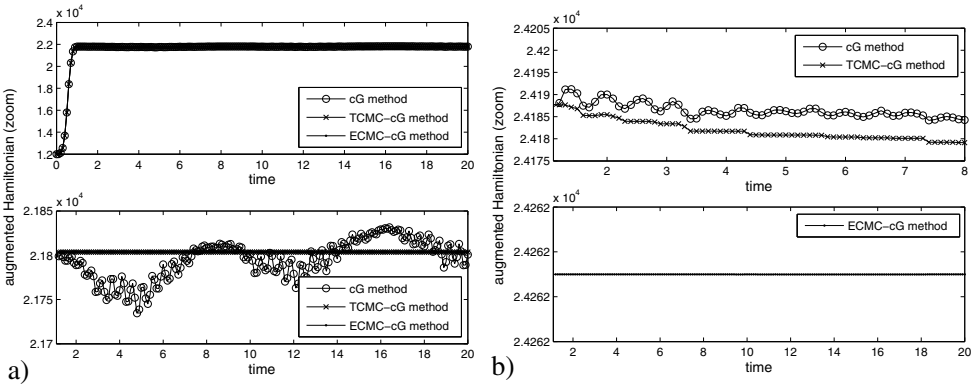

Figure 5: Augmented Hamiltonian $H + D$: a) purely elastic case, b) plastic case

for the chosen parameters the Newmark scheme is related to the (undamped) trapezoidal rule and the 'HHT method' has been specifically designed to provide a numerically dissipative behaviour. Once more, the 'Flying Frame' has been used for the computations, whereby the initial setup remains unchanged, only the applied parameters have been altered: $\lambda = 500$, $\mu = 250$, $Y_0 = 40$, $H = 100$, $\rho = 3.0$, $f_{max} = 20$, and $T_{load} = 1.0$. Moreover, small as well as large time-step sizes have been applied to assess fairly the offered performance of the different time-stepping schemes and, additionally, the time-step sizes have been changed during the calculation, namely from $h_n = 0.02$ to $h_n = 0.06$ respectively from $h_n = 0.1$ to $h_n = 0.3$ after $t = 2.2$, to check the robustness of the integrators. A sequence of the motion, including contour plots of the hardening variable, can be regarded in Fig. 11 and the local evolution of the hardening parameter is pictured exemplarily for two points of the frame in Fig. 12. However, in the following, special emphasis is placed on the resulting consistency properties. Considering Fig. 8, the accumulated dissipation D is, once more, (strictly) non-negative due to the chosen local update and the results of the different integrators are qualitatively similar, especially if small time-step

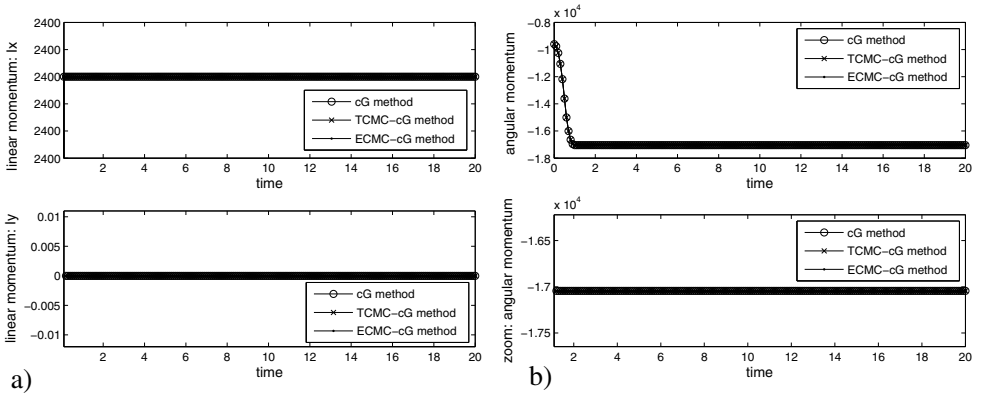

Figure 6: Momentum maps: a) linear momentum $\boldsymbol{I}$ (elastic case), b) component of the angular momentum $\boldsymbol{L}$ (plastic case)

sizes are applied. Nevertheless, the results differ quantitatively, whereby the application of the 'HHT method' results in the lowest physical dissipation, which seems to be significantly underestimated when dealing with large time-step sizes. Moreover, the differences in the total energy H between the classical integrators and the Galerkin-based 'ECMC-cG method' are quite impressive, compare Fig. 7. It can be clearly seen that the standard integrators are not able at all to feature a physically correct monotonic decrease of the total energy. Rather, both classical integration schemes suffer from oscillations in the total energy which increase drastically for large time-step sizes, especially if the widespread Newmark method is applied. One might think that such aspects are only of theoretical interest, but in fact, on the one hand, a physically correct time integration is essential for a qualitatively correct simulation of the dynamical behaviour and, on the other hand, the evolution of the total energy is directly related to the robustness of the integrators. This accepted fact is also confirmed by the present example, since the application of the Newmark method results in a critical energy blow-up when large time-step sizes are taken into account [3], compare Fig. 7 b). Contrariwise, the 'HHT method' offers an unphysical decrease of the total energy caused by its numerically dissipative character. Please note furthermore, that this strong decrease of the total energy is not accompanied by a high physical dissipation D, as discussed above. To investigate the relation between the decrease of the total energy and the increase of the accumulated (physical) dissipation in detail, the augmented Hamiltonian $H + D$ is plotted in Fig. 9. Once more, the results of both standard integrators show an unphysical behaviour which is characterised by oscillations and an increase respectively decrease of the augmented Hamiltonian. Solely, the 'ECMC-cG method' captures the conservation of the augmented Hamiltonian, respecting the energy balance (20). Furthermore, the standard integrators violate the conservation of angular momentum, whereas the Galerkin-based scheme features the mechanical consistency, as pictured in Fig. 10. It is important to emphasise that the abovementioned consistency properties of the 'ECMC-cG method' are guaranteed for small as well as for large time-step sizes,

[3] A program abort within the calculations is displayed by means of a vertical dashed line in the plots.

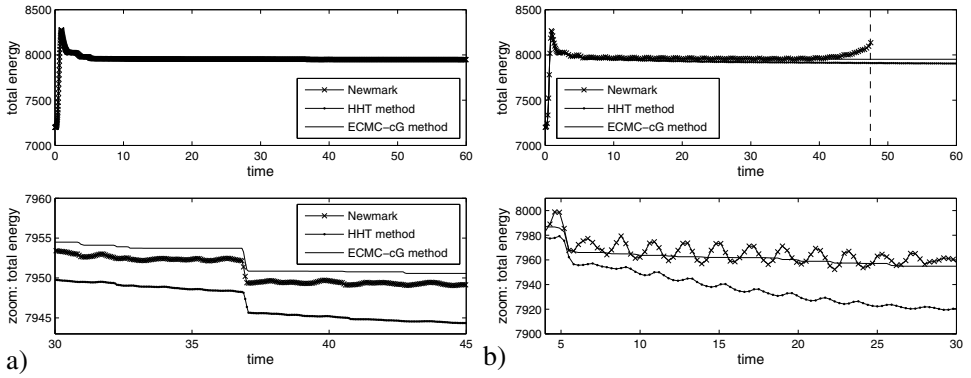

Figure 7: Total energy H: a) small time-step size, b) large time-step size

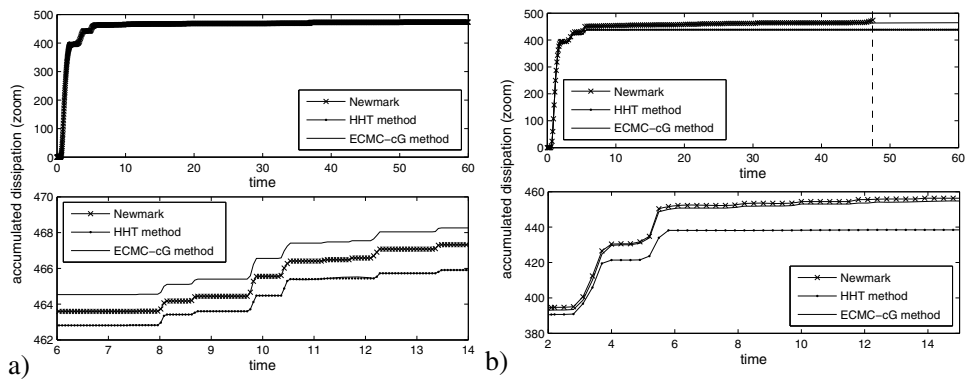

Figure 8: Accumulated dissipation D: a) small time-step size, b) large time-step size

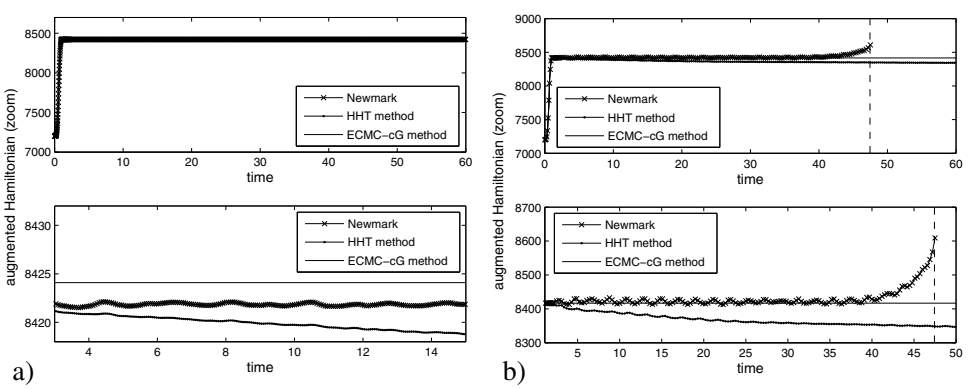

Figure 9: Augmented Hamiltonian $H + D$: a) small time-step size, b) large time-step size

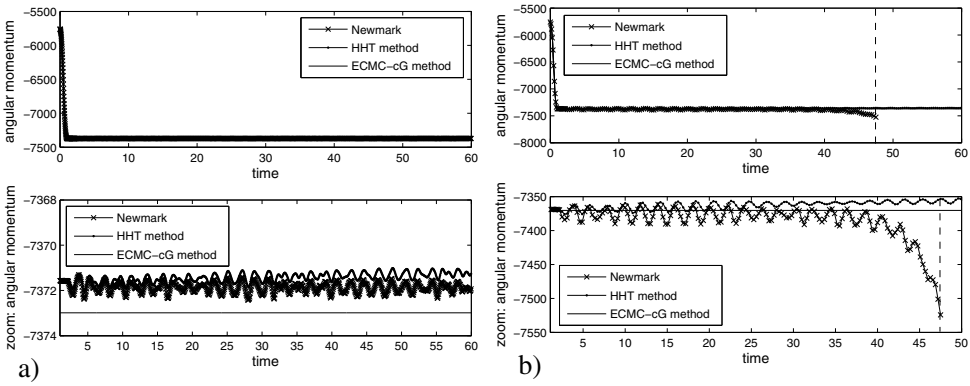

Figure 10: Component of the angular momentum $\boldsymbol{L}$: a) small time-step size, b) large time-step size

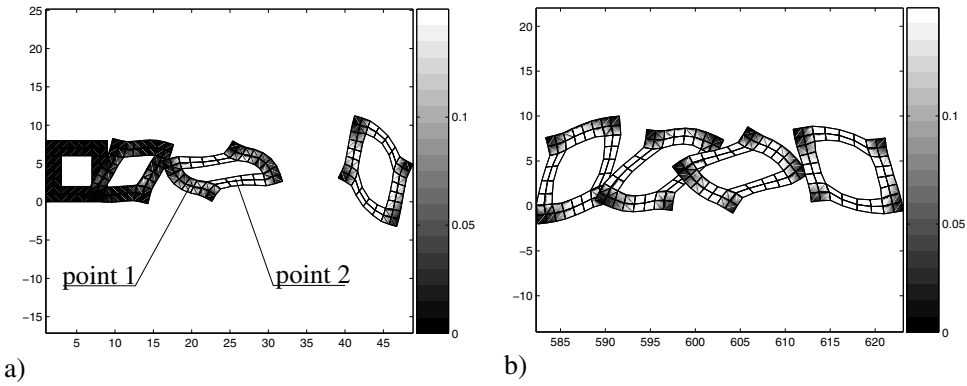

Figure 11: Contour plot of the hardening parameter (large time-step size): a) $t \in \{0.1, 0.8, 2, 4\}$, b) $t \in \{58.3, 59.2, 60.1, 61.3\}$

unaffected by changes of the step size during the calculation. Consequently, the proposed consistent Galerkin-based integration schemes enable an exceedingly robust integration of finite elasto-plasto-dynamics that is of particular importance for long-time simulations.

5 Conclusions

In the present paper, we have proposed time integration algorithms based on Finite Elements in time for nonlinear dynamics including plastic deformations, whereby the kinematic description of the applied plasticity model adopts a multiplicative decomposition of the deformation gradient into an elastic and a plastic part. With regard to a physically correct integration, nonstandard quadrature rules are required to feature thermodynamical

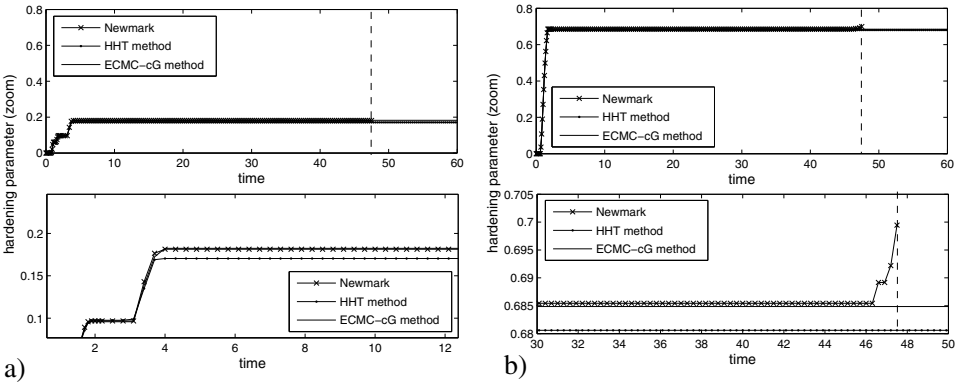

Figure 12: Evolution of the hardening parameter (large time-step size) in: a) point 1, b) point 2

consistency respectively energy-consistency. In this context, special emphasis has been placed on the assessment of the resulting schemes, especially, in comparison to classical integrators which are in particular well-established for linear (elastic) dynamical systems. Thereby, the superior performance of the proposed methods has been clearly confirmed, whereby particularly the 'ECMC-cG method' covers essential conservation properties of the continuum formulation for elastic as well as for plastic deformations. Recapitulating, Galerkin-based time-stepping schemes combined with adequate quadrature rules are also preeminently appropriate for geometrically nonlinear elasto-plasto-dynamics, providing an excellent numerical performance with pre-defined conservation properties.

Acknowledgements Financial support by the German Research Foundation DFG within the International Research Training Group 1131 'Visualization of Large and Unstructured Data Sets. Applications in Geospatial Planning, Modeling, and Engineering' is gratefully acknowledged by the authors.

References

[Arm05] F. Armero. Energy-dissipative momentum-conserving time-stepping algorithms for dynamic finite strain plasticity. In Proceedings of *COMPLAS VIII – International Conference on Computational Plasticity*, Barcelona, 2005.

[Arm06] F. Armero. Energy-dissipative momentum-conserving time-stepping algorithms for finite strain multiplicative plasticity. *Computer Methods in Applied Mechanics and Engineering*, 195:4862–4889, 2006.

[AZ06] F. Armero, C. Zambrana. Numerical integration of the nonlinear dynamics of elasto-plastic solids. In *Computational Mechanics – Solids, Structures and Coupled Problems*, 127–146, Springer, 2006.

[BB99] O. Bauchau, C. Bottasso. On the design of energy preserving and decaying schemes for flexible, non-linear multi-body systems. *Computer Methods in Applied Mechanics and Engineering*, 169:61–79, 1999.

[BS00a] P. Betsch, P. Steinmann. Inherently energy conserving time finite elements for classical mechanics. *Journal of Computational Physics*, 160:88–116, 2000.

[BS00b] P. Betsch, P. Steinmann. Conservation properties of a time FE method. Part I: Time-stepping schemes for N-body problems. *International Journal for Numerical Methods in Engineering*, 49:599–638, 2000.

[BS01] P. Betsch, P. Steinmann. Conservation properties of a time FE method. Part II: Time-stepping schemes for nonlinear elastodynamics. *International Journal for Numerical Methods in Engineering*, 50:1931–1955, 2001.

[Bot97] C. Bottasso. A new look at finite elements in time: a variational interpretation of Runge-Kutta methods. *Applied Numerical Mathematics*, 25:355–368, 1997.

[BBT01a] M. Borri, C. Bottasso, and L. Trainelli. Integration of elastic multibody systems by invariant conserving/dissipating algorithms. i. Formulation. *Computer Methods in Applied Mechanics and Engineering*, 190:3669–3699, 2001.

[BBT01b] C. Bottasso, M. Borri, and L. Trainelli. Integration of elastic multibody systems by invariant conserving/dissipating algorithms. ii. Numerical schemes and applications. *Computer Methods in Applied Mechanics and Engineering*, 190:3701–3733, 2001.

[EEHJ96] K. Eriksson, D. Estep, P. Hansbo, and C. Johnson. *Computational Differential Equations*. Cambridge University Press, 1996.

[Gonz00] O. Gonzalez. Exact energy and momentum conserving algorithms for general models in nonlinear elasticity. *Computer Methods in Applied Mechanics and Engineering*, 190:1763–1783, 2000.

[GBS05] M. Gross, P. Betsch, and P. Steinmann. Conservation properties of a time FE method. Part IV: Higher order energy and momentum conserving schemes. *International Journal for Numerical Methods in Engineering*, 63:1849–1897, 2005.

[HHT77] H. Hilber, T. Hughes, R. Taylor. Improved numerical dissipation for time integration algorithms in structural dynamics. *Earthquake Engineering & Structural Dynamics*, 5:283–292, 1977.

[Hug87] T. Hughes. *The Finite Element Method*. Prentice-Hall, New Jersey, 1987.

[KC99] D. Kuhl, M. Crisfield. Energy-conserving and decaying algorithms in non-linear structural mechanics. *International Journal for Numerical Methods in Engineering*, 45:569–599, 1999.

[Lee69] E. Lee. Elastic-plastic deformation at finite strains. *Journal of Applied Mechanics*, 36:1–6, 1969.

[ML02a] X. Meng, T. Laursen. Energy consistent algorithms for dynamic finite deformation plasticity. *Computer Methods in Applied Mechanics and Engineering*, 191:1639–1675, 2002.

[ML02b] X. Meng, T. Laursen. On energy consistency of large deformation plasticity models, with application to the design of unconditionally stable time integrators. *Finite Elements in Analysis and Design*, 38:949–963, 2002.

[MMS06a] R. Mohr, A. Menzel, and P. Steinmann. Galerkin-based time integrators for geometrically nonlinear elasto-plastodynamics – Challenges in modeling and visualization. In *Visualization of Large and Unstructured Data Sets, GI-Edition Lecture Notes in Informatics (LNI)*, S-4:185–194, 2006.

[MMS07a] R. Mohr, A. Menzel, and P. Steinmann. Conservation properties of Galerkin-based time integrators for geometrically nonlinear elasto-plasto-dynamics. In Proceedings of *IMPLAST – Symposium on Plasticity and Impact Mechanics*, Bochum, 2007.

[MMS07b] R. Mohr, A. Menzel, and P. Steinmann. Conservation properties of Galerkin-based time-stepping schemes for finite elasto-plasto-dynamics. In Proceedings of *COMPLAS IX – International Conference on Computational Plasticity*, Barcelona, 2007.

[MMS07c] R. Mohr, A. Menzel, and P. Steinmann. A consistent time-FE method for large strain elasto-plasto-dynamics. Submitted for publication, 2007.

[New59] N. Newmark. A method of computation for structural dynamics. *ASCE Journal of the Engineering Mechanics Division*, 85:67–94, 1959.

[NSP06] L. Noels, L. Stainier, and J. Ponthot. An energy momentum conserving algorithm using the variational formulation of visco-plastic updates. *International Journal for Numerical Methods in Engineering*, 65:904–942, 2006.

[ST92] J. Simo, N. Tarnow. The discrete energy-momentum method. Conserving algorithms for nonlinear elastodynamics. *Zeitschrift fuer Angewandte Mathematik und Physik (ZAMP)*, 43:757–792, 1992.

[Sim98] J. Simo. Numerical analysis and simulation of plasticity. In *Handbook of Numerical Analysis*, 6:183–499, 1998.